

1

2

3 **IMPROVING THE COMPLEMENTARY METHODS TO ESTIMATE**
4 **EVAPOTRANSPIRATION UNDER DIVERSE CLIMATIC AND**
5 **PHYSICAL CONDITIONS**

6

7 Fathi M. Anayah¹ and Jagath J. Kaluarachchi²

8 ¹ Utah Water Research Laboratory
9 Utah State University
10 Logan, UT 84322-8200
11 fathi.anayah@aggiemail.usu.edu
12 *Corresponding author*

13

14

15 ² College of Engineering
16 Utah State University
17 Logan, UT 84322-4100
18 jkalu@engineering.usu.edu

19

20 **March 2014**

21

22
23
24
25
26
27
28
29
30
31
32
33
34
35
36
37
38
39
40
41
42
43

ABSTRACT

Reliable estimation of evapotranspiration (ET) is important for the purpose of water resources planning and management. Complementary methods, including Complementary Relationship Areal Evapotranspiration (CRAE), Advection-Aridity (AA) and Granger and Gray (GG), have been used to estimate ET because these methods are simple and practical in estimating regional ET using meteorological data only. However, prior studies have found limitations in these methods especially in contrasting climates. This study aims to develop a calibration-free universal method using the complementary relationships to compute regional ET in contrasting climatic and physical conditions with meteorological data only. The proposed methodology consists of a systematic sensitivity analysis using the existing complementary methods. This work used 34 global FLUXNET sites where eddy covariance (EC) fluxes of ET are available for validation. A total of 33 alternative model variations from the original complementary methods were proposed. Further analysis using statistical methods and simplified climatic class definitions produced one distinctly improved GG-model based alternative. The proposed model produced a single-step ET formulation with results equal or better than the recent studies using data-intensive, classical methods. Average root mean square error (RMSE), mean absolute bias (BIAS) and R^2 across 34 global sites were 20.57 mm/month, 10.55 mm/month and 0.64, respectively. The proposed model showed a step forward toward predicting ET in large river basins with limited data and requiring no calibration.

Keywords: Evapotranspiration; Complementary methods; FLUXNET; Global model.

44

45

1. INTRODUCTION

46 A reliable estimate of ET in river basins is important for the purpose of water resources planning
47 and management. ET represents a significant portion of rainfall in the water balance especially in
48 semi-arid regions where most rainfall is typically lost as ET (FAO, 1989). Therefore, the
49 uncertainty in estimating ET can lead to the inaccurate prediction of water balance. A careful
50 screening of available meteorological, land use/land class and related hydrologic data in typical
51 rural river basins suggest that ET is more challenging to calculate given the limited data. Data
52 limitations in most rural river basins highlighted the importance of using alternative methods as
53 opposed to the classical methods using land use/land cover data. While remote sensing
54 techniques are available to estimate ET, such methods are expensive and necessary data may not
55 be readily available for verification (Jimenez et al., 2011). Complementary methods initially
56 proposed by Bouchet (1963) and others are alternative methods that can be used to calculate ET
57 using meteorological data such as relative humidity, temperature and sunshine hours.

58 There are several classical methods presently available to estimate potential ET whereas
59 estimating actual ET requires detailed local data such as land cover/land use, crop pattern and
60 growing cycle. Typically, these classical methods predict crop ET from crop covered areas
61 during the growing season to manage agricultural water demands. Crop ET is nothing but the
62 potential ET multiplied by an appropriate crop coefficient, which is sometimes called the two-
63 step approach (Allen et al., 1998). However, the actual water loss from the land surface is not
64 restricted to crop areas only; instead evaporation happens from open water bodies as well as
65 from open land surfaces with minimal vegetation cover. In water resources planning, the

66 important estimate is the total water loss from the land surface that may or may not include
67 transpiration from crop areas.

68 For several decades, complementary methods, including CRAE (Morton, 1983), AA (Brutsaert
69 and Stricker, 1979) and GG (Granger and Gray, 1989) methods, have been used to estimate ET
70 or total water loss from the land surface independent of land cover. These methods are attractive
71 due to simplicity and practicability in estimating ET, wet environment ET (ETW) and potential
72 ET (ETP) at the regional scale using meteorological data only. Previous studies attempted to use
73 the complementary methods with little success (Doyle, 1990; Hobbins et al., 2001; McMahon et
74 al., 2013; Szilagyi and Kovacs, 2010; Xu and Singh, 2005) given the limited understanding of
75 the methods and the conflicting definitions of different terms. Still the complementary methods
76 offer a distinct advantage over the classical methods given the simplicity, ready availability of
77 required data and the ability to estimate total water loss as opposed to crop ET only.

78 Any improvements to the complementary methods cannot be conducted without the use of actual
79 ET measurements. As a part of this study, it is important to use measured ET data for model
80 validation. Currently, ET fluxes are directly measured using the eddy covariance (EC) method
81 that uses surface energy fluxes for weather forecasting and hydrologic modeling. These fluxes
82 include sensible heat (H) and latent heat (LE) fluxes. Compared to other methods such as
83 lysimeters, an EC system produces minimal physical disturbance to the surrounding environment
84 and captures the areal fluxes within the footprint area (Luo et al., 2010). Most importantly, EC
85 data are freely accessible worldwide, for example, FLUXNET (<http://fluxnet.ornl.gov/>) which is
86 a global network of micrometeorological sites that use the EC methods to measure land-
87 atmosphere exchange of carbon dioxide, water vapor and energy fluxes (Baldocchi et al., 2001).
88 FLUXNET comprises of free-access regional networks such as AmeriFlux, AsiaFlux, EuroFlux

89 and CarboAfrica. Given the task of finding a large set of global data with different climatic
90 conditions and physical conditions, this study used the FLUXNET sites similar to many other
91 studies (Castellvi and Snyder, 2010; Huntington et al., 2011).

92 The major limitation of the EC method is the lack of energy balance closure (i.e., $H + LE \neq R_n -$
93 G_{soil} where R_n is net radiation and G_{soil} is soil heat flux) that causes underestimation of ET
94 (Wilson et al., 2002). Twine et al., (2000) and Wang et al. (2008) showed that underestimation of
95 ET can be as high as 15%, however, others, Castellvi et al. (2008); Huntington et al. (2011) and
96 Wilson et al. (2002), found lower percentages within measurement uncertainty that can be <5%.
97 These studies showed that the impact of energy imbalance in the EC method may not be
98 significant as thought earlier (Castellvi and Snyder, 2010). Hence, the EC method is still
99 attractive and served as the standard method for direct measurement of ET fluxes (Castellvi et
100 al., 2008; Luo et al., 2010).

101 Hobbins et al. (2001) and Xu and Singh (2005) found limitations to the complementary methods
102 in different physical and climatic conditions especially in arid settings. Some of these limitations
103 lead to many unanswered questions such as; how applicable are the complementary relationship
104 to estimate ET? Are these methods only valid within humid climates? What are the limitations in
105 the different complementary methods? Have complementary methods been compared to
106 measured ET data under a variety of climatic and physical conditions? Given these unanswered
107 questions, it is important to address the validity of the complementary methods in a scientifically
108 justifiable manner.

109 It is found that there is no single study where the ET estimates from the complementary methods
110 have been extensively predicted and evaluated using data from EC sites. To evaluate the

111 applicability of the complementary methods and to propose suitable changes, the methods need
112 to be evaluated under a variety of land cover/land use classes and climatic conditions. In
113 addition, the three complementary methods, CRAE, AA and GG, have not been cross-compared
114 and evaluated using measured ET data. Therefore the goals of this study are to investigate the
115 applicability of the complementary methods in estimating ET in contrasting environments,
116 perform necessary revisions to the existing methods to improve estimates if necessary and finally
117 propose a universal model of estimating ET that is calibration-free, simple, robust and uses
118 minimum data.

119 2. COMPLEMENTARY METHODS

120 2.1 Complementary Relationship

121 Complementary methods describe the relationships between ET, ETW and ETP using the
122 complementary relationship first introduced by Bouchet (1963). The theory states that a
123 complementary relationship exists between ET and ETP as shown in Fig. 1 (see Davenport and
124 Hudson, 1967; Pettijohn and Salvucci, 2009). ETW, however, is ET that would occur if the soil-
125 plant surface is wet enough so that ET could approach its potential value, ETP (Granger, 1989).
126 The development of the complementary relationships **and the definitions of various terms are**
127 **discussed in detail** by Brutsaert and Stricker (1979), Granger and Gray (1989), Lhomme and
128 Guilioni (2006), McMahon et al. (2013), Morton (1983) and Pettijohn and Salvucci (2009). The
129 three definitions of ET are related as

$$130 \quad ET = 2ETW - ETP \quad (1)$$

131 where ET, ETW and ETP are in mm/month. Equation (1) which is the Bouchet original
132 expression indicates that an increase in ET is accompanied by an equivalent decrease of ETP,

133 i.e., $\delta ET = -\delta ETP$. In other words, as the surface dries, actual ET decreases causing a reduction
134 in humidity and an increase in temperature of the surrounding air, and as a result ETP will
135 increase. Once ETP and ETW are estimated, ET is subsequently derived.

136 In the literature, the complementarity relationship between ET and ETP shown in Eq. (1) is of
137 controversy among scientists who claimed that many inherent assumptions of Bouchet theory
138 lack sufficient evidence (Granger, 1989; Lhomme and Guilioni, 2006). Recently, there have been
139 several attempts to improve the complementary relationship and its predictive power of different
140 ET definitions (see Brutsaert and Stricker, 1979; Granger and Gray, 1989; Morton, 1983). Han et
141 al. (2012) developed a nonlinear approach to the complementary relationship but the results
142 require further study and verification. Yet, Lhomme and Guilioni (2010) proposed a different
143 model that can describe the complex relationship between ET and ETP based on the convective
144 boundary layer.

145 **2.2 CRAE Method**

146 ETP is estimated by solving the energy balance and vapor transfer equations iteratively (Morton,
147 1983). ETP is calculated by solving at equilibrium temperature (T_p in $^{\circ}C$) at which the energy
148 balance and vapor transfer equations for a moist surface are equivalent. The procedure describing
149 the iterative solution is given by Morton (1983, Appendix C). The energy balance equation to
150 estimate ETP is given as

$$151 \quad ETP = R_T - \lambda f_T (T_p - T) \quad (2)$$

152 where R_T is net radiation for soil-plant surfaces (mm/month) at air temperature T ($^{\circ}C$), λ is the
153 heat transfer coefficient (mbar/ $^{\circ}C$) and f_T is the vapor transfer coefficient (mm/month/mbar). To

154 estimate ETW in Eq. (4), net radiation for soil-plant surfaces at T_p (R_{TP}) is first computed using
155 Eq. (3).

$$156 \quad R_{TP} = ETP + \gamma f_T (T_p - T) \quad (3)$$

$$157 \quad ETW = b_1 + b_2 (1 + \gamma / \Delta_p)^{-1} R_{TP} \quad (4)$$

158 where γ is the psychrometric constant (mbar/°C), b_1 is a constant representing advection energy,
159 b_2 is a constant and Δ_p is the rate of change of saturation vapor pressure with T at T_p (mbar/°C).
160 Constants b_1 and b_2 were calibrated using climatic data from arid regions in North America and
161 Africa (Morton, 1983). ETP from Eq. (2) and ETW from Eq. (4) are used in Eq. (1) to calculate
162 ET of the CRAE method.

163 **2.3 AA Method**

164 In the AA method, Penman (1948) equation (ET_{PEN}) is used to estimate ETP as shown in Eqs.
165 (5) and (6).

$$166 \quad ET_{PEN} = \frac{\Delta}{\gamma + \Delta} (R_n - G_{soil}) + \frac{\gamma}{\gamma + \Delta} E_a \quad (5)$$

$$167 \quad E_a = 10.6 \times (\beta + 0.54U)(e_s - e_a) \quad (6)$$

168 where Δ is rate of change of saturation vapor pressure with T (mbar/°C), R_n is net radiation
169 (mm/month), G_{soil} is soil heat flux (mm/month), E_a is drying power of air (mm/month), β is a
170 constant and usually equals to 1.0, U is wind speed at 2 m above ground level (m/s), e_s is
171 saturation vapor pressure at T (mm Hg) and e_a is vapor pressure of air (mm Hg). In the wind
172 formulation of Penman (1956), β was updated to 0.5. Although both wind function formulae
173 (when $\beta = 1$ or 0.5) are widely used in hydrology, Penman preferred β of 1 (see Brutsaert and

174 Stricker, 1979; McMahon et al., 2013). Brutsaert and Stricker (1979) mentioned that their
175 method is insensitive to the wind function. The first term of Eq. (5) is called equilibrium ET and
176 the second is aerodynamic ET that is generated by large scale advection effects (see Hobbins et
177 al., 2001). When advection is minimal, the interactions of atmosphere with the soil-plant system
178 will be completely developed and an equilibrium condition is approached (Brutsaert and
179 Stricker, 1979).

180 ETW of the AA method is calculated using ET_{PT} of Priestley and Taylor (1972) in which
181 minimal advection is assumed and given by Eq. (7).

$$182 \quad ET_{PT} = \alpha \frac{\Delta}{\gamma + \Delta} (R_n - G_{soil}) \quad (7)$$

183 where α is a coefficient that typically equals to 1.26 or 1.28 (Priestley and Taylor, 1972). The
184 AA method in this study used α of 1.28 and β of 1. ETP from Eq. (5) and ETW from Eq. (7) are
185 used in Eq. (1) to calculate ET of the AA method.

186 **2.4 GG Method**

187 The complementary relationship given in Eq. (1) is primarily used by the CRAE and AA
188 methods. In the GG method, Granger and Gray (1989) used a modified version as shown in Eq.
189 (8).

$$190 \quad ET = (1 + \frac{\gamma}{\Delta})ETW - \frac{\gamma}{\Delta}ETP \quad (8)$$

191 Equation (8) is reduced to Eq. (1) only when $\gamma = \Delta$. In this method, two new concepts were
192 proposed and empirically correlated together; relative drying power (D) and relative evaporation
193 (G) shown in Eqs. (9) and (10), respectively.

194
$$D = \frac{E_a}{E_a + (R_n - G_{\text{soil}})} \quad (9)$$

195
$$G = \frac{ET}{ETP} \quad (10)$$

196 where D indicates surface dryness, i.e., D becomes larger as the surface becomes drier. G is ET
 197 that occurs under similar wind and humidity conditions from a saturated surface at the actual
 198 temperature (Granger and Gray, 1989).

199 In the original work, G was defined as G_1 through Eq. (11) where this equation was empirically
 200 derived using data from two stations in a semi-arid region of Western Canada. Granger and Gray
 201 (1989) mentioned that G_1 is independent of land use.

202
$$G_1 = \frac{1}{c_1 + c_2 e^{c_3 D}} \quad (11)$$

203 where $c_1=1.0$, $c_2=0.028$ and $c_3=8.045$. In the GG method, the selection of the function to
 204 calculate relative evaporation (G) has great impact on the actual ET estimates and any
 205 modification to this empirical formula may be significant in improving the predictability of the
 206 GG method. In essence, there is more research required in this effort. Thus, Eq. (11) was later
 207 modified by Granger (1998) to account for different surface conditions as shown in Eq. (12).

208
$$G_2 = \frac{1}{c_4 + c_5 e^{c_6 D}} + c_7 D \quad (12)$$

209 where $c_4=0.793$, $c_5=0.2$, $c_6=4.902$ and $c_7=0.006$. Therefore G in Eq. (10) can be substituted by G_1
 210 of Eq. (11) or G_2 of Eq. (12).

211 ETW required to solve Eq. (8) is obtained from Eq. (5) earlier used in the AA model. Thereafter
212 G_1 is used in Eq. (10) together with Eq. (9) to solve for ET in Eq. (8). The final equation
213 describing ET in the GG method is therefore given as

$$214 \quad ET = \frac{\Delta G}{\gamma + \Delta G} (R_n - G_{soil}) + \frac{\gamma G}{\gamma + \Delta G} E_a \quad (13)$$

215 where ET, R_n , G_{soil} and E_a are in mm/month. Although the CRAE, AA and GG methods enable
216 the direct prediction of ET without the need for surface parameters (temperature and vapor
217 pressure), but the GG method is the only method that does not require a prior estimate of ETP
218 (Granger, 1989).

219 **2.5 Alternative method (ASCE)**

220 In the popular ASCE method (Allen et al., 2005), input data to calculate net radiation (R_{ASCE}) are
221 similar to those of the CRAE method. More specifically, the ASCE method requires minimum
222 and maximum temperature data, which sometimes are not available. In such a case the procedure
223 described by Allen et al. (2005, Eq. (E.5)) is followed. One major difference between the CRAE
224 and ASCE methods is the albedo calculation. In the former, albedo is calculated using a set of
225 equations whereas albedo is fixed at 0.23 in the latter. The ASCE method also requires wind
226 speed measurements to calculate ETP while estimating crop ET requires detailed information of
227 land cover/land use, crops, cropping pattern and the growing cycle. The ASCE method is
228 specifically utilized in this study to compare R_{ASCE} with R_T and R_{TP} . The ASCE method is also
229 used to calculate G_{soil} using monthly averages of temperature data.

230

3. MEASURED FLUX AND METEOROLOGICAL DATA

231 3.1 Sites of EC Data

232 In this study 34 global sites were selected with measured meteorological and flux data and these
233 sites are distributed as follows: 17 from AmeriFlux sites, 11 from EuroFlux sites, five from
234 AsiaFlux sites and one CarboAfrica site (see Fig. 2). Unfortunately, efforts to obtain data from
235 other sites in CarboAfrica have not been successful. The selection of the 34 sites was based on
236 data availability and climatic variability. The details of the sites and data collected are shown in
237 Table 1 and Fig. 2.

238 The reason to select 34 sites is that prior studies have typically used less number of sites and in
239 most cases under similar climatic conditions. By using a variety of global sites in contrasting
240 physical and climatic conditions with measured ET data, we will demonstrate the validity of the
241 proposed complementary method in different land use/land class categories. While there are
242 other EC global sites, these sites could not be considered due to the lack of diversity of land
243 classes and climatic conditions required in this study. As mentioned earlier, data accessibility
244 was also an issue in some cases.

245 To classify the climatic conditions prevailing at each site, a simple aridity index developed by De
246 Martonne (1925), AI_M (in mm/°C), is chosen and given as

$$247 \quad AI_M = \frac{P_{ann}}{T_{ann} + 10} \quad (14)$$

248 where P_{ann} is average annual precipitation in mm and T_{ann} is average annual T in °C. Unlike other
249 aridity indices, AI_M indicates the availability of both water and energy from readily available
250 data. In effect, the sites were sorted to the following climatic classes; very humid ($AI_M \geq 35$),

251 humid ($28 \leq AI_M < 35$), sub-humid ($24 \leq AI_M < 28$), Mediterranean ($20 \leq AI_M < 24$), semi-arid
252 ($10 \leq AI_M < 20$) and arid ($AI_M < 10$).

253 As shown in Table 1, the 34 sites have different geographic and climatic conditions. The dataset
254 consists of 1657 monthly measurements across the 34 sites. The P_{ann} values range from 196 mm
255 at site 25 to 2231 mm at site 4, and T_{ann} varies between -1.7 °C at site 3 and 26.3 °C at site 4. It is
256 noticed that many sites fall within the very humid climatic class. The surface conditions also
257 differ considerably from grasslands to forests. Data are available from 12 to 120 months from
258 1992 to 2010. At site 1, for example, data from 24 months are available in 2006 and 2007, while
259 at site 4 there are no ET data in April 2003. Therefore, the total number of months included in
260 the calculations from 2002 to 2005 is 47 instead of 48.

261 The EC tower heights vary from 2 m at site 24 to 103 m at site 14 with a median value of 10 m at
262 site 7 and an average value of 17.1 m. The EC tower height reflects the vertical flux footprint
263 that usually indicates the upwind area captured by the instruments mounted on the tower.
264 Starting from very humid, humid, sub-humid, Mediterranean, semi-arid to arid climatic classes,
265 the average EC tower heights are 24.8, 28.2, 15.8, 10.2, 4.6 and 6.8 m, respectively. It is no
266 surprise that the tower heights are highest in the very humid sites where the land cover is
267 dominated by forests of high canopy altitudes. However, low tower heights are required for arid
268 and semi-arid sites naturally characterized by grass or shrub land covers. The high range of EC
269 tower heights explains the suitability of selecting these particular 34 EC sites that have flux
270 footprints of the scale of the complementary methods. This observation may lead to the
271 conclusion that a perfect correlation between the EC and complementary methods may exist.

272 Compared to the lowest average ET_{EC} flux (10.5 mm/month) that occurs at site 25, site 4 has the
273 maximum of 134.3 mm/month. It is observed that site 4 has the highest ET_{EC} fluxes across the 34
274 sites because the site is located in tropical peat swamp forests where soil moisture is relatively
275 high throughout the year (Hirano et al., 2005) and the site is also exposed to high energy
276 demands. In general, the wide ranges of ET_{EC} fluxes and AI_M values reflect the diversity of
277 hydrologic and climatic conditions present in this study.

278 **3.2 Measured Flux Data from EC Systems**

279 In comparison to finer resolution data, collecting data at monthly scale is easier in rural and
280 sparse areas, less problematic when data quality is poor and more appropriate for regional-scale
281 studies. Thompson et al. (2011) examined model performance using different time scales from
282 half hourly to inter-annual and found that a monthly time step is preferable. Data in this study
283 were directly downloaded from its regional network website and sometimes obtained (or
284 complemented) through personal communications. In cases where monthly data were not readily
285 available, average monthly data were aggregated from finer time resolution data, e.g., daily or
286 hourly. To keep minimal changes to the input data, months of available data (50% or more) only
287 were considered in the analysis.

288 Input data requirements are often the driver to select a specific method to estimate ET. Even in
289 rural regions where data limitations are common, data to calculate R_n from the CRAE method
290 (Morton, 1983) requires monthly averages of temperature, humidity (or dew-point temperature)
291 and sunshine hours (or solar radiation) only. Again, the CRAE method calculates two types of
292 R_n ; R_T and R_{TP} at the same time. It is obvious that the CRAE method can also estimate ETP,
293 ETW and ET using the same data. However, both AA and GG methods, similar to any classical
294 method, need wind speed measurements to calculate ET (see Eq. 6).

295 The performance indicators used to assess the model predictions are root mean square error
296 (RMSE), mean absolute bias (BIAS) and coefficient of determination (R^2). As the number of
297 sites is large, the absolute value of mean bias (BIAS), which indicates the disparity of predicted
298 and measured ET, is preferred over the mean bias value itself because negative values of mean
299 bias cannot cancel positive values.

300 **4. MODEL DEVELOPMENT AND RESULTS**

301 The approach used here is a systematic model sensitivity analysis across the three existing
302 complementary methods to identify the major model components contributing to predicting ET
303 compared to the EC observations. The findings from each step of the sensitivity analysis is later
304 used to propose a universal model that is calibration-free and capable of predicting ET (or total
305 water loss) independent of land cover/use. The proposed approach can be divided into four
306 stages: (1) First, the three original complementary methods are applied across all 34 sites to
307 identify the relative accuracy of each method, (2) Using the results obtained from the first stage,
308 a set of model variations representing the different model structures will be developed, (3) Next
309 the model variations with acceptable results will be selected for further analysis and (4) Finally, a
310 statistical analysis will be conducted to differentiate between the final model(s) to identify a
311 universal model capable of predicting ET across all sites without calibration. To further test the
312 proposed model, the results of this study will be compared with the results of recently published
313 ET studies.

314 **4.1 Comparison between Original Complementary Methods**

315 The ET estimates computed using the three original complementary methods were compared to
316 the measurements from the EC sites (ET_{EC}) and the results are given in Table 2. It is no surprise

317 that the sub-humid climatic class has the poorest performance as there are only two sites in this
318 class of which site 19 has the poorest values of RMSE, BIAS and R^2 . For the CRAE method, the
319 sites with arid climates have the lowest RMSE and BIAS values and sites with wet (very humid
320 and humid) climates have the highest R^2 values. The AA method was developed for a watershed
321 experiencing severe drought, and therefore, this method is expected to outperform the other two
322 methods in arid climates. Hobbins et al. (2001) evaluated the CRAE and AA methods across 120
323 basins in the United States. They found that as aridity increases, the CRAE method tends to
324 overestimate ET and the AA method tends to underestimate ET. Xu and Singh (2005) evaluated
325 three sites of diverse climates and found that the predictive power of the methods increases with
326 humidity. This conclusion contradicts with the results in Table 2 as the CRAE and AA methods
327 perform best in arid climates. In general, the three methods work relatively well under extreme
328 climatic conditions, either arid or humid. Also the predictions of the GG method are slightly
329 better in humid climates than arid as found by Xu and Singh (2005). Overall, the CRAE method
330 is the best according to RMSE and R^2 while the GG method has the lowest BIAS. Still, the
331 computed ET estimates are not close enough to the ET_{EC} measurements indicating that there is a
332 need for improvements to the existing methods.

333 **4.2 Development of Alternative Model Variations**

334 The prior estimates of ET are highly dependent on R_n . Net radiation computed by Morton (1983)
335 is denoted as R_T which is net radiation at T while R_{TP} is net radiation at T_p . Net radiation from
336 Allen et al. (2005) is denoted as R_{ASCE} . When compared to the R_n measurements from the EC
337 sites, the three estimates of net radiation perform better as humidity increase. Although detailed
338 results are not shown here, the average R^2 values of R_T and R_{ASCE} estimates range from 88% to
339 98% and from 92 to 98%, respectively. While R_{ASCE} is the overall best estimator of R_n , R_T

340 performs better in arid and semi-arid regions. The results of this analysis clearly indicate that the
341 net radiation prediction is dependent on the climatic class and therefore, any improvements
342 should consider climate dependency.

343 Selecting the correct equations to calculate ETP, ETW and even ET may significantly influence
344 the accuracy of the net radiation estimates. This work used the original model equations of the
345 CRAE, AA and GG methods in different ways. This study is not meant to explore all possible
346 relationships between ETP and ETW; instead the focus here is developing a reliable predictive
347 model of actual ET that is applicable under a variety of climatic and physical conditions.
348 Therefore, the relationships and model equations of the original methods were used here in a
349 manner to preserve the physical processes controlling ET. Similarly, there are two formulae to
350 describe the complementary relationship, namely equations (1) and (8). It is true that there may
351 be other possible formulae to simulate the complementary relationship between ET, ETW and
352 ETP. The drawback of these approaches is the need for calibration for which the revised model
353 will be applicable for a given site or region. This condition is against the original purpose of this
354 study that attempts to develop a model that is widely applicable for many different climatic and
355 physical conditions.

356 In Stage 2, different combinations of model formulations are considered to develop a set of
357 alternative model variations that may be better than the original methods. For instance, these
358 alternative model variations can decide if R_T is a better estimator of net radiation compared to
359 R_{ASCE} or not. Similarly another question is if the complementary relationships are adequately
360 presented by Eq. (1) or Eq. (8) or a different formulation is needed. In selecting these different
361 alternative model variations, the criteria for the sensitivity analysis used are; the method to
362 calculate R_n , the representation of the complementary relationship, the value of α in the ET_{PT}

363 equation, the value of β in the wind function of the ET_{PEN} equation and the relative evaporation
364 function (G) of the GG method. After studying the model structure of each complementary
365 method, 17 different alternative model variations are proposed in Table 3 for subsequent
366 analysis. As discussed earlier, this is a systematic parameter sensitivity exercise to identify the
367 best alternative model variation. Although more model variations are possible, the 17 listed
368 alternative model variations are adequate at this stage. For example, the AA and GG methods
369 have four criteria each (R_n , complementary relationships, α and β) producing 16 model
370 variations. An important consideration in the development of these model variations is the
371 conclusions of others. For instance, Hobbins et al. (2001) found that changes to the AA method
372 did not necessarily produce superior results especially by perturbing β (see Brutsaert and
373 Stricker, 1979).

374 The ET estimates produced by these 17 alternative model variations across the 34 sites were
375 compared to the EC measurements and the results are shown in Fig. 3. It should be noted that
376 Fig. 3 shows the anomalies from the original method for each model variation. In effect, the
377 results are considered to show improvements if the anomaly of RMSE is negative. The same
378 trend is valid for BIAS but opposite for R^2 . It is observed that none of the CRAE- or AA-based
379 alternative model variations improved RMSE and BIAS. Among the CRAE-based model
380 variations, CRAE2 has the minimum deterioration of RMSE and BIAS while showing some
381 improvement of R^2 . A similar behavior is noticed with AA4 of the AA-based model variations.
382 However, the GG-based model variations have obvious improvements across all three metrics.
383 GG1, GG3, GG5 and GG7 model variations showed improved RMSE and BIAS values when
384 compared with the original GG method. The only common feature among these four GG model
385 variations is Eq. (1) representing the complementary relationship and not Eq. (8) which was used

386 by the original GG method. This observation indicates that Eq. (1) is superior in representing the
387 complementary relationships between ET, ETW and ETP. The deterioration of results in the GG-
388 based model variations is deemed minor when compared to other model variations. The
389 conclusion from Stage 2 is that these GG model variations perform better than the CRAE and
390 AA model variations.

391 Although ETP is usually given under saturated conditions by in the equation of Penman (1948)
392 as shown in the original AA method, yet the definition of ETW still has some ambiguity
393 (Lhomme and Guilioni, 2006). One important difference of the original GG method compared to
394 the other two methods is the equation describing ETW. ETW of the original CRAE and AA
395 methods is derived from the ET_{PT} equation (Eq. (7)) while the original GG method uses the
396 ET_{PEN} equation or Eq. (5) (Brutsaert and Stricker, 1979; Granger and Gray, 1989; Morton, 1983).
397 Given this departure of the GG model from others, we further studied the GG model variations
398 based on the model describing ETW. Accordingly, another set of alternative model variations
399 from the GG model is possible. These variations consist of 16 models (GG8 through GG23) and
400 the details are given in Table 4. In these variations, β is no longer changed while α in the ET_{PT}
401 equation will be changed. ETW in all these variations will use the Priestley-Taylor equation
402 (Table 4). In total, 24 GG model variations (GG1 through GG23 from Tables 3 and 4) are now
403 considered for the next stage.

404 **4.3 Selection of Best Performing GG Model Variation**

405 For the purpose of selecting the best GG model variation(s), each model from the latest 24 was
406 run and the results were compared with EC observations (see Table 5). The performance metrics
407 were used to identify the best GG model variation in each climatic and performance metric
408 combination and the results are shown in Table 5. For example, GG3 was the best for RMSE,

409 GG1 for BIAS and GG17 and GG23 for R^2 in the Very Humid class. In essence, 11 GG model
410 variations became eligible from the 24 selected earlier from Stage 2. It is also observed that
411 GG20 is the best for six combinations of performance metric and climatic class combinations. In
412 contrast, GG3 is the best only in RMSE for the Very Humid class. GG1, GG3, GG11 and GG13
413 are the best models each for one combination of metric and climatic class combination only.
414 Therefore these GG model variations were rejected and the remaining seven (GG7, GG14,
415 GG17, GG18, GG20, GG22 and GG23) were selected for further consideration.

416 There are other key observations made from the prior analysis. First, the original GG method
417 uses the complementary relationship given by Eq. (8) (Granger, 1989), yet, five of the seven
418 promising model variations selected earlier uses Eq. (1). In essence, this observation suggests
419 that Eq. (1) is better in capturing the variability of ET compared to Eq. (8). Second, six of these
420 seven promising GG model variations use ET_{PT} equation to calculate ETW. Third, a comparison
421 between R_T and R_{ASCE} shows that six of these promising GG model variations use R_{ASCE} to
422 denote net radiation that supports the conclusion drawn earlier. Fourth, five of these GG model
423 variations use Eq. (12) to calculate G. Lastly, changing the value of α in the ET_{PT} equation and
424 varying the equation describing G did not alter the results.

425 The next step of the analysis will be to identify the best model variation of the seven selected
426 earlier. Before proceeding to the next step, the six climatic classes are simplified to represent
427 climatic variability using three simple classes; wet (from original very humid and humid),
428 moderate (from original sub-humid and Mediterranean) and dry (from original semi-arid and
429 arid). This revision shall not affect the results and will make the analyses and conclusions
430 simple. Using these new definitions, the original 34 global sites are now reallocated as 18, 6 and
431 10 into wet, moderate and arid classes, respectively.

432 Figure 4 shows the results of performance metrics to these seven models using the simplified
433 climatic classes of wet, moderate and dry. For all climatic classes, GG17 has the highest RMSE
434 and GG7 has the highest BIAS values. GG7 performs well only in the wet climatic class, while it
435 performs poor in the moderate and dry classes. The GG17 and GG23 model variations have
436 identical behaviors since these differ in the α value only. Both models fail in the moderate
437 climatic class. It is also noticed that GG14 does not simulate ET well in the moderate climatic
438 class.

439 Overall, GG22 has the lowest median and average values of RMSE that are 16.20 and 20.23
440 mm/month, respectively. These results indicate that GG22 has the potential to be the best model
441 variation. Based on BIAS for all sites, the lowest average value is 10.55 mm/month for GG18,
442 while the lowest median value is 7.45 mm/month for GG20. Comparing the three model
443 variations, both GG18 and GG20 have same R^2 of 0.64 and GG22 produced 0.62. It is therefore
444 reasonable to state that GG18, GG20 and GG22 are the best GG model variations for further
445 consideration.

446 There is no evidence to suggest that a specific model variation from these three models is
447 superior in a particular climatic class. The climatic class with poorest performance is the
448 moderate class. The reason may be the low number of sites in this class and therefore extreme
449 values such as those of site 24 can dramatically influence the results. In the moderate climatic
450 class, GG22 has the lowest average RMSE and BIAS, however, GG18 and GG20 share the
451 highest average R^2 . It is also noted that all three model variations have the following similarities;
452 net radiation is calculated by R_{ASCE} , the complementary relationship is represented by Eq. (1)
453 and the ETW is computed by Eq. (7).

454 The performance metrics (RMSE, BIAS and R^2) for the three model variations can be compared
455 with uncertainty associated with observed EC-based fluxes to assess the overall accuracy of the
456 methods. For example, Mauder et al. (2007) showed that RMSE and bias of LE sensors normally
457 range from 38 to 61 mm/month and from -29 to 30 mm/month, respectively. In another study, it
458 was found that EC data are comparable to weighing lysimeter ET measurements (Castellvi and
459 Snyder, 2010) when the RMSE was 26 mm/month and R^2 was 0.98. These results indicate the
460 high efficiency of the three model variations, namely GG18, GG20 and GG22, in predicting the
461 actual ET.

462 **4.4 Statistical Analysis**

463 The applicability of the three GG model variations, GG18, GG20 and GG22, is further
464 investigated using the analysis of variance (ANOVA) to assess if these three models are similar
465 or not (Berthouex and Brown, 2002). The ANOVA test was used on the time-series consisting of
466 1657 estimates of ET from each model variation and measured ET_{EC} . The average values of ET
467 across the 34 sites are 35.9, 33.8, 33.2 and 32.0 mm/month, for GG18, GG20, GG22 and
468 measured data, respectively. There is a tendency to underestimate average ET by all three model
469 variations. The reason may be the similarity in structure of the three GG model variations. The
470 ANOVA F-test statistic ($F_{V1,V2,1-CI}$) was computed for the four time-series (simulated 3 GG
471 model variations and ET_{EC} observations) at 95% confidence level (V1 is number of models
472 minus 1, V2 is number of measurements – number of models and CI is confidence interval) and
473 compared to that of the F test of ANOVA. Simply, if the F test is smaller, methods are alike. In
474 this case, $F_{3,1653,0.05}$ is found to be 2.60 (Berthouex and Brown, 2002, Table C in Appendix) while
475 the F test is 4.58. Therefore, it is obvious at 95% confidence, the averages of the four time series

476 are not equal; however, the test cannot identify which model variation is different compared to
477 the others.

478 For this purpose, Dunnet's method (Berthouex and Brown, 2002) was used to compare the three
479 GG model variations to the measured ET_{EC} fluxes. The Dunnet's method has the advantage to
480 answer two questions; a confidence interval in which average values are alike and the direction
481 of the difference. The results of the Dunnet's method showed that at 95% confidence interval,
482 the average ET is between 32.3 and 39.4 mm/month. In other words, GG22 is statistically
483 different while the difference in each of the other two model variations is likely to be
484 insignificant. Figure 5 shows the average ET estimates across 33 sites according to the climatic
485 class. At site 4, none of the models can simulate the elevated ET fluxes measured. In general,
486 GG22 underestimates ET as humidity increases. However, the scatter of data around the 1:1 line
487 for most climatic classes is more pronounced with GG18 and GG20. The similarity between
488 GG18 and GG20 is visible because the only difference between the two models is α in the ET_{PT}
489 equation that does not influence the results. In fact, GG18 has two advantages over the other two
490 model variations; it has the closest average ET value to that of the ET_{EC} fluxes and closest to the
491 1:1 line (see Fig. 5). Hence, GG18 is deemed to be the best from the seven promising GG model
492 variations.

493 In Fig. 6, the performance metrics of GG18 are shown for each site in the three climatic classes.
494 The R^2 values have a minor increasing trend with humidity. The R^2 values at sites of wet climatic
495 class mostly lie above the average value and vice versa for the dry climatic class. There is no
496 such trend with RMSE and BIAS. However, the RMSE and BIAS values at most sites of the dry
497 climatic class are below the average value. Again, it is emphasized that site 4 has specific data
498 issues that have to be further inspected. Generally, Fig. 6 demonstrates that GG18 is consistently

499 predicting ET across these 34 sites that have diverse climatic and physical conditions. It also
500 indicates that there is no evidence that the flux footprint (EC tower height) plays a major role or
501 directly impacts the accuracy of the results.

502 The average R^2 values of GG18 over the wet, moderate and dry classes are 0.72, 0.61 and 0.52,
503 respectively. Since the ET fluxes differ between the wet and dry climates, the absolute values of
504 RMSE may not be simply compared to each other. Instead, the RMSE value at each site is
505 divided by the average ET_{EC} value shown in Table 1 such that the relative RMSE is computed
506 and compared across all sites. The values of relative RMSE for GG18 range from 0.23 at site 11
507 to 1.59 at site 34 with an average of 0.69.

508 **4.5 Comparison with Recent Studies**

509 In this section, the results of the proposed modified complementary method, specifically GG18,
510 are compared to the results from recently published studies using the classical methods and
511 original complementary methods.

512 Suleiman and Crago (2004) estimated hourly ET using radiometric surface temperatures in two
513 grassland sites in Oklahoma and Kansas and validated using EC data. The results showed the
514 RMSE values ranging from 32 to 53 mm/month while R^2 varied between 0.78 and 0.94. Mu et
515 al., (2007) used data from 19 AmeriFlux EC sites to validate the estimates of a remotely sensed
516 ET using a revised Penman-Monteith equation. The average RMSE, bias and R^2 were 29
517 mm/month, -6 mm/month and 0.76, respectively. When used with 46 AmeriFlux sites (Mu et al.,
518 2011), the results showed average RMSE, absolute bias and R^2 of 26 mm/month, 10 mm/month
519 and 0.65, respectively. Kuske (2009) estimated ET using Penman-Monteith and Priestley-Taylor
520 equations and compared estimates to EC data. Both models were significantly overestimating the

521 high ET fluxes and slightly underestimating the low ET fluxes. Thompson et al. (2011) tested ET
522 “null” model that couples the Penman-Monteith equation to a soil moisture model at 14
523 AmeriFlux sites from which eight sites are used in the present study. RMSE varied between 56
524 and 208 mm/month and therefore, changes were made to further improve the model to produce
525 RMSEs of 34 to 175 mm/month.

526 However, complementary methods to predict ET have not been extensively compared with EC-
527 based ET measurements. With the exception of Ali and Mawdsley (1987), researchers have
528 recently started paying attention to the complementary methods. A monthly ET map using a
529 modified Morton method was produced using MODIS imagery for Hungary (Szilagyi and
530 Kovacs, 2010) and verified using three EC sites. At two sites, R^2 values were 0.79 and 0.80 and
531 bias ranged between -19 mm/month and 21 mm/month. At the third site, however, the authors
532 found a difference of 44% with the EC measurements **due to physical conditions at that**
533 **particular EC tower (see Szilagyi and Kovacs, 2010)**. Shifa (2011) examined the wind function
534 of the AA model using data under wet and dry conditions. With the original AA method, RMSE
535 was 17 mm/month and 29 mm/month for the wet and dry conditions, respectively. The author
536 found that the AA method performs best using calibrated wind function coefficients under wet
537 conditions in which RMSE and R^2 were 12 mm/month and 0.7, respectively. Huntington et al.
538 (2011) tested the AA method using data from arid shrublands at five EC sites in Eastern Nevada.
539 It was found that RMSE, R^2 and percent bias were 13 mm/month, 0.77 and 18%, respectively.
540 RMSE, R^2 and percent bias of a modified AA method were 11 mm/month, 0.71 and 1%,
541 respectively. Han et al. (2011) proposed an enhanced GG model at four sites under different land
542 covers and compared to the original GG method and EC-based ET data. The enhanced model

543 was better than the original GG method at three sites and RMSE of the enhanced GG model
544 ranged from 4 to 16 mm/month.

545 Table 6 shows the results from a set of the abovementioned studies compared with the results of
546 the proposed GG18 model variation. The comparison shows that the results of the GG18 model
547 variation are equal or better and more reliable considering the wide range of physical and
548 climatic conditions of the 34 global EC sites used in this study. More importantly, the ET
549 estimates of GG18 outperform the estimates of ET of other studies given the minimal cost and
550 data needed to compute reliable regional ET using meteorological data only. Furthermore, GG18
551 is a single-step method that does not require local calibration and therefore suitable to use in
552 rural river basins with minimal data and monitoring while providing the total water loss from the
553 land surface that is appropriate in water resources planning.

554 The GG18 model is close to a “universal model” and shows better behavior among the 34 sites
555 and the results are more consistent across the spectrum of climatic classes as shown in Fig. 6.
556 The ET estimates of the GG18 model for the moderate-climate sites are comparable to both wet
557 or dry climatic classes (Fig. 6), and those of the most recent ET studies (Table 6). None of the
558 original (CRAE, AA and GG) methods, however, succeeded to estimate ET under sub-humid
559 and Mediterranean climatic classes (see Table 2). The discrepancy is clear when compared to the
560 more extreme conditions, i.e., dry and humid categories (Table 2). For example, one may argue
561 that the average values of performance metrics of the GG18 model are slightly better than those
562 of the original CRAE method that does not need wind measurements. The comparison cannot be
563 made only between the overall average values given by the CRAE method and the GG18 model.
564 There are other statistics (e.g., standard deviation) that show the accuracy (or distribution) of the
565 ET estimates among the 34 sites. As discussed earlier, one major problems of the CRAE method

566 is that it fails to estimate ET under sub-humid and Mediterranean climatic classes (see Table 2).
567 Under the diverse physical and climatic conditions, the GG18 model variation is quantitatively
568 and qualitatively outperforming all original complementary method. The model structure of the
569 proposed GG18 model variation is given in Fig. 7.

570 One last concern is about the most proper temporal resolution of the GG18 model. It is known
571 that the original AA and GG methods are usually used at daily timescale while the original
572 CRAE method is typically used at monthly timescale. The goal of this study is to propose a
573 universal ET model that can be successfully used for data deficit conditions under which daily
574 data are missing or unavailable. It is believed that the regional estimates of ET entail monthly
575 time resolution. Thus, the question now is whether applying the GG18 model at monthly
576 timescale may change the parameters of the model used at daily basis or not. In order to answer
577 this question, the proposed GG18 model was applied to a countrywide study of Ghana where
578 daily data were available and climate varies from semi-arid in the north to tropical humid in the
579 south (Anayah et al., 2013). The predictions using monthly data from 2000 to 2005 were very
580 much comparable to the daily estimates of the GG18 model. These results suggested that the
581 GG18 model can accommodate both daily and monthly time steps to produce consistent results.
582 The reader may refer to Anayah (2012) and Anayah et al. (2013) for further details.

583 **5. SUMMARY AND CONCLUSIONS**

584 Complementary methods have the potential to predict regional ET using minimal meteorological
585 data. However, prior studies used small data sets representing limited climatic variability and
586 physical conditions that were not successful in improving the methods. A few of the successful
587 studies used locally calibrated parameters that may not have the universal applicability simply
588 due to the two-step approach required to compute ET. In addition, water resources studies

589 require the total water loss from the land surface irrespective of the land use/land class. In this
590 regard, complementary methods provide the distinct advantage over the classical methods that
591 only provide crop ET using detailed input data such as land use/land class, cropping patterns and
592 crop calendar. The state of the complementary methods is such that there is no single
593 methodology consistently used over a wide variety of climatic and physical conditions. This
594 study is aimed at developing calibration-free universal model using the complementary
595 relationship that requires meteorological data only to predict regional ET.

596 In this work, 34 global sites with measured ET data via the EC method are used to develop the
597 proposed model using systematic sensitivity analysis conducted with the three original
598 complementary methods. The sites have different climatic and physical conditions to ensure the
599 universal application of the proposed model. The three original complementary methods
600 consisting of CRAE, AA and GG are first evaluated and the need for improvement to all
601 methods is determined. Based on the model structures, 20 alternative model variations are
602 proposed. The GG method was found to be the most attractive compared to the other two
603 methods and therefore the GG method is further analyzed. ETW that uses Priestley-Taylor
604 equation produced 16 GG model variations. Climates of the FLUXNET sites were initially sorted
605 to six climatic classes based on the aridity index proposed by De Martonne (1925). The initial
606 results identified seven promising model variations. Given the complexity of using six different
607 climatic classes, the analysis later reduced this number to three distinct climatic classes
608 consisting of wet, moderate and dry climates. This simplification identified three promising
609 model variations from the earlier seven variations. Statistical analyses conducted via ANOVA
610 testing and the Dunnett method showed that two of the model variations are similar while one GG
611 model variation, GG18, clearly provided a different distribution and results. Therefore the GG18

612 model variation was considered the best. Also the comparison of results from recent studies
613 showed that the GG18 model variation is capable of producing equal or better results while
614 capturing a wide variety of physical and climatic conditions.

615 In the proposed GG18 model, net radiation R_n is computed using R_{ASCE} calculated by Allen et al.
616 (2005) which outperforms R_T developed by Morton (1983). It is evident that the simple
617 complementary relationships suggested by Eq. (1) can describe the behavior of ET fluxes better
618 than the more generic complementary relationship of Eq. (8). Most importantly, the predictive
619 power of the GG method (Granger and Gray, 1989) is improved when the ET_{PT} equation is used
620 to calculate ETW. There is a strong indication that the proposed GG18 model can significantly
621 enhance the accuracy of ETW using the GG method and consequently to predict regional ET
622 using meteorological data only and without calibration. Furthermore, this one-step estimation
623 method can reliably estimate ET regardless of the prevailing climatic conditions. Such an
624 estimate will unequivocally lead to reliable predictions of water resources, in particular recharge
625 estimation and impacts due to climate change.

626 **6. ACKNOWLEDGEMENTS**

627 This study was supported by the Utah Water Research Laboratory of Utah State University with
628 additional funding available from the International Water Management Institute, Sri Lanka. We
629 thank Drs. Vladimir Smakhtin and Paul Pavelic for their support and encouragement. The
630 authors would like to acknowledge all scientists of FLUXNET agencies and Naama Raz-Yaseef
631 from University of California, Berkeley for their willingness to share data. The assistance of Drs.
632 David Stevens, Luis Bastidas and David Tarboton from Utah State University is appreciated. The
633 English of the manuscript had been kindly edited by Naomi Higham.

634

7. REFERENCES

635 Ali, M. F. and Mawdsley, J. A.: Comparison of two recent models for estimating actual ET using
636 only regularly recorded data, *J. Hydrol.*, 93, 257-276, [doi:10.1016/0022-1694\(87\)90099-0](https://doi.org/10.1016/0022-1694(87)90099-0),
637 1987.

638 Allen, R. G., Pereira, L. S., Raes, D. and Smith, M. (Eds.): *Crop Evapotranspiration: Guidelines*
639 *for Computing Crop Water Requirements*, FAO Irrig. Drain., Paper No. 56, Food and Agr.
640 Orgn. of the United Nations, Rome, Italy, 1998.

641 Allen, R. G., Walter, I. A., Elliot, R., Howell, T., Itenfisu, D. and Jensen, M. (Eds.): *The ASCE*
642 *Standardized Reference Evapotranspiration Equation*, Environment and Water Resources
643 Institute of the Am. Soc. Civil Eng. (ASCE), Task Committee on Standardization of
644 Reference Evapotranspiration, Final Rep., ASCE, Reston, VA, USA, 2005.

645 Anayah, F. M.: *Improving complementary methods to predict evapotranspiration for data deficit*
646 *conditions and global applications under climate change*, Ph.D. dissertation, Utah State
647 University, Logan, Utah, USA, 186 pp., 2012.

648 Anayah, F. M., Kaluarachchi, J. J., Pavelic, P., and Smakhtin, V.: *Predicting groundwater*
649 *recharge in Ghana by estimating evapotranspiration*, *Water International*, 38(4), 408-432,
650 [doi: 10.1080/02508060.2013.82164](https://doi.org/10.1080/02508060.2013.82164), 2013.

651 Baldocchi, D., Falge, E., Gu, L., Olson, R., Hollinger, D., Running, S., Anthoni, P., Bernhofer,
652 C., Davis, K., Evans, R., Fuentes, J., Goldstein, A., Katul, G., Law, B., Lee, X., Malhi, Y.,
653 Meyers, T., Munger, W., Oechel, W., Paw, K. T., Pilegaard, K., Schmid, H. P., Valentini, R.,
654 Verma, S., Vesala, T., Wilson, K., and Wofsy, S.: *FLUXNET: A New Tool to Study the*
655 *Temporal and Spatial Variability of Ecosystem-Scale Carbon Dioxide, Water Vapor, and*

656 Energy Flux Densities, B. Am. Meteorol. Soc., 82, 2415–2434, doi:10.1175/1520-
657 0477(2001)082<2415:FANTTS>2.3.CO;2, 2001.

658 Berthouex, P. and Brown, L. (Eds.): Statistics for Environmental Engineers, second ed., Lewis
659 publishers, CRC Press LLC, FL, USA, 2002.

660 Bouchet, R. J.: Evapotranspiration réelle et potentielle, signification climatique, in: General
661 Assembly Berkeley, Int. Assoc. Sci. Hydrol., Gentbrugge, Belgium, Publ. No. 62, 134-142,
662 1963.

663 Brutsaert, W., and Stricker, H.: An Advection Aridity Approach to Estimate Actual Regional
664 Evaporation, Water Resour. Res., 15(2), 443-450, doi:10.1029/WR015i002p00443, 1979.

665 Castellvi, F., and Snyder, R. L.: A comparison between latent heat fluxes over grass using a
666 weighing lysimeter and surface renewal analysis, J. Hydrol., 381, 213-220, doi:
667 10.1016/j.jhydrol.2009.11.043, 2010.

668 Castellvi, F., Snyder, R. L., and Baldocchi, D. D.: Surface energy-balance closure over rangeland
669 grass using the eddy covariance method and surface renewal analysis, Agr. Forest Meteorol.,
670 148, 1147-1160, doi: 10.1016/j.agrformet.2008.02.012, 2008.

671 Davenport, D. C. and Hudson, J. P.: Changes in evaporation rates along a 17-km transect in the
672 Sudan Gezira, Agr. Meteorol., 4, 339-352, 1967.

673 De Martonne, E. (Eds.): Traité de Géographie Physique, tome 1, fourth ed., A. Colin, Paris,
674 1925.

675 Doyle, P.: Modelling catchment evaporation: an objective comparison of the Penman and
676 Morton approaches, J. Hydrol., 121, 257-276, 1990.

677 FAO (Eds.): Arid zone forestry: A guide for field technicians, FAO Conservation Guide 20,
678 Food and Agr. Org. of the United Nations, Rome, Italy, 1989.

679 Granger, R. J.: A complementary relationship approach for evaporation from nonsaturated
680 surfaces, *J. Hydrol.*, 111, 31-38, doi: 10.1016/0022-1694(89)90250-3, 1989.

681 Granger, R. J.: Partitioning of energy during the snow-free season in the Wolf Creek research
682 basin, in: *Proceedings of the Wolf Creek Research Basin - Hydrology, Ecology, Environment*
683 *workshop*, Whitehorse, Yukon, Canada, 5-7 March 1998, 33-44, 1998.

684 Granger, R. J., and Gray, D. M.: Evaporation from natural nonsaturated surfaces, *J. Hydrol.*, 111,
685 21-29, doi: 10.1016/0022-1694(89)90249-7, 1989.

686 Han, S., Hu, H., Yang, D. and Tian, F.: A complementary relationship evaporation model
687 referring to the Granger model and the advection–aridity model, *Hydrol. Process.*, 25, 2094-
688 2101, doi: 10.1002/hyp.7960, 2011.

689 Han, S., Hu, H. and Tian, F.: A nonlinear function approach for the normalized complementary
690 relationship evaporation model, *Hydrol. Process.*, 26, 3973-3981, doi: 10.1002/hyp.8414,
691 2012.

692 Hirano, T., Segah, H., Limin, S., June, T., Tuah, S. J., Kusin, K., Hirata, R. and Osaki, M.:
693 Energy balance of a tropical peat swamp forest in Central Kalimantan, Indonesia, *Phyton*,
694 45(4), 67-71, 2005.

695 Hobbins, M. T., Ramirez, J. A., Brown, T. C., and Claessens, L. H.: The complementary
696 relationship in estimation of regional evapotranspiration: The Complementary Relationship
697 Areal Evapotranspiration and Advection-Aridity models, *Water Resour. Res.*, 37(5), 1367-
698 1387, doi: 10.1029/2000WR900358, 2001.

699 Huntington, J. L., Szilagyi, J., Tyler, S. W., and Pohl, G. M.: Evaluating the complementary
700 relationship for estimating evapotranspiration from arid shrublands, *Water Resour. Res.*, 47,
701 W05533, doi: 10.1029/2010WR009874, 2011.

702 Jimenez, C., Prigent, C., Mueller, B., Seneviratne, S. I., Mc-Cabe, M. F., Wood, E. F., Rossow,
703 W. B., Balsamo, G., Betts, A. K., Dirmeyer, P. A., Fisher, J. B., Jung, M., Kanamitsu, M.,
704 Reichle, R. H., Reichstein, M., Rodell, M., Sheffield, J., Tu, K., and Wang, K.: Global inter-
705 comparison of 12 land surface heat flux estimates, *J. Geophys. Res.*, 116, D02102, doi:
706 10.1029/2010JD014545, 2011.

707 Kuske, T. J.: Fluxes of energy and water vapour from grazed pasture on a mineral soil in the
708 Waikato, M.Sc. thesis, The Univ. of Waikato, New Zealand, 152 pp., 2009.

709 Lhomme, J. P., and Guilioni, L.: Comments on some articles about the complementary
710 relationship, *J. Hydrol.*, 323(1-4), 1-3, doi:10.1016/j.jhydrol.2005.08.014, 2006.

711 Lhomme, J. P., and Guilioni, L.: On the link between potential evaporation and regional
712 evaporation from a CBL perspective, *Theor. Appl. Climatol.*, 101,143-147, doi:
713 10.1007/s00704-009-0211-0, 2010.

714 Luo, X., Wang, K., Jiang, H., Sun, J., Xu, J., Zhu, Q., and Li, Z.: Advances in research of land
715 surface evapotranspiration at home and abroad, *Sciences in Cold and Arid Regions*, 2(2),
716 0104-0111, 2010.

717 Mauder, M., Oncley, S. P., Vogt, R., Weidinger, T., Ribeiro, L., Bernhofer, C., Foken, T.,
718 Kosiek, W., De Bruin, H. A. R., and Liu, H.: The energy balance experiment EBEX-2000,
719 Part II: Intercomparison of eddy-covariance sensors and post-field data processing methods,
720 *Bound. Layer Meteorol.*, 123, 29-54, doi: 10.1007/s10546-006-9139-4, 2007.

721 McMahon, T. A., Peel, M. C., Lowe, L., Srikanthan, R., and McVicar, T. R.: Estimating actual,
722 potential, reference crop and pan evaporation using standard meteorological data: a
723 pragmatic synthesis, *Hydrol. Earth Syst. Sc.*, 17(4), 1331-1363, doi:10.5194/hess-17-1331-
724 2013, 2013.

725 Morton, F. I.: Operational estimates of areal evapotranspiration and their significance to the
726 science and practice of hydrology, *J. Hydrol.*, 66, 1-76, doi:10.1016/0022-1694(83)90177-4,
727 1983.

728 Mu, Q., Heinsch, F. A., Zhao, M., and Running, S. W.: Development of a global
729 evapotranspiration algorithm based on MODIS and global meteorological data, *Remote Sens.*
730 *Environ.*, 111(4), 519-536, doi: 10.1016/j.rse.2007.04.015, 2007.

731 Mu, Q., Zhao, M., and Running, S. W.: Improvements to a MODIS global terrestrial
732 evapotranspiration algorithm, *Remote Sens. Environ.*, 115, 1781-1800, doi:
733 10.1016/j.rse.2011.02.019, 2011.

734 Penman, H. L.: Natural evaporation from open water, bare soil, and grass, *Roy. Soc. London*,
735 *Ser. A*, 193, 120-145, doi:10.1098/rspa.1948.0037, 1948.

736 Penman, H. L.: Evaporation: An introductory survey, *Neth. J. Agr. Sci.*, 4, 9-29, 1956.

737 Pettijohn, J. C., and Salvucci, G. D.: A New Two-Dimensional Physical Basis for the
738 Complementary Relation between Terrestrial and Pan Evaporation, *J. Hydrometeorol.*, 10(2),
739 565-574, doi: <http://dx.doi.org/10.1175/2008JHM1026.1>, 2009.

740 Priestley, C. H. B., and Taylor, R. J.: On the assessment of surface heat flux and evaporation
741 using large-scale parameters, *Mon. Weather Rev.*, 100, 81-92, doi:10.1175/1520-
742 0493(1972)100<0081:OTAOSH>2.3.CO;2, 1972.

743 Shifa, Y. B.: Estimation of evapotranspiration using advection aridity approach, M.Sc. thesis,
744 University of Twente, The Netherlands, 52 pp., 2011.

745 Suleiman, A. and Crago, R.: Hourly and daytime ET from grassland using radiometric surface
746 temperatures, *Agron. J.*, 96, 384-390, 2004.

747 Szilagyi, J., and Kovacs, A.: Complementary-relationship-based evapotranspiration mapping
748 (cremap) technique for Hungary, *Periodica Polytech.*, 54(2), 95-100, doi:
749 10.3311/pp.ci.2010-2.04, 2010.

750 Thompson, S. E., Harman, C. J., Konings, A. G., Sivapalan, M., Neal, A., and Troch, P. A.:
751 Comparative hydrology across AmeriFlux sites: The variable roles of climate, vegetation,
752 and groundwater, *Water Resour. Res.*, 47, W00J07, doi: 10.1029/2010WR009797, 2011.

753 Twine, T., Kustas, W. P., Norman, J. M., Cook, D. R., Houser, P. R., Meyers, T. P., Prueger, J.
754 H., Starks, P. J., and Wesely, M. L.: Correcting eddy-covariance flux underestimates over a
755 grassland, *Agr. Forest Meteorol.*, 103, 279-300, doi:10.1016/S0168-1923(00)00123-4, 2000.

756 Wang, T., Sammis, W. and Miller, D. R.: Eddy covariance measurements of crop water uses: the
757 energy closure problem and potential solutions, in: *Agricultural Water Management*
758 *Research Trends*, Nova Science Publishers Inc., New York, USA, 1-7, 2008.

759 Wilson, K., Goldstein, A., Falge, E., Aubinet, M., Baldocchi, D., Berbigier, P., Bernhofer, C.,
760 Ceulemans, R., Dolman, H., Field, C., Grelle, A., Ibrom, A., Law, B. E., Kowalski, A.,
761 Meyers, T., Moncrieff, J., Monson, R., Oechel, W., Tenhunen, J., Valentini, R., and Verma,
762 S.: Energy balance closure at FLUXNET sites, *Agr. Forest Meteorol.*, 113, 223-243, doi:
763 10.1016/S0168-1923(02)00109-0, 2002.

764 Xu, C. Y., and Singh, V. P.: Evaluation of three complementary relationship evapotranspiration
765 models by water balance approach to estimate actual regional evapotranspiration in different
766 climatic regions, *J. Hydrol.*, 308, 105-121, doi:10.1016/j.jhydrol.2004.10.024, 2005.

767

Tables
Table 1. Characteristics of the 34 EC sites with measured ET data used in the study.

#	Site	Country	Lat. °	Long. °	Height m	Data availability	ET _{EC} , mm/month			AI _M mm/°C	Land cover
						from-to (# months)	min	mean	max		
Very humid											
1	Takayama	Japan	36.1	137.4	25	06-07 (24)	9.4	44.4	91.7	83.2	Deciduous forest
2	Walker Branch, TN	USA	36	-84.3	44	95-98 (48)	10.5	47.4	116.2	76.5	Deciduous forest
3	Qinghai	China	37.6	101.3	2.2	02-04 (36)	1.6	36.2	110.5	68.3	Alpine meadow
4	Palangkaraya	Indonesia	2.3	114	41.3	02-05 (47)	82.4	134.3	164	61.5	Tropical forest
5	Harvard Forest, MA	USA	42.5	-72.2	30	92-99 (96)	5.1	37.5	108.4	61.2	Mixed forest
6	Flakaliden	Sweden	64.2	19.8	15	96-98 (31)	-0.1	23	63.4	51.5	Coniferous forest
7	Bondville, IL	USA	40	-88.3	10	97-06 (120)	1.7	50.1	135.4	49.6	Cropland
8	Goodwin Creek, MS	USA	34.3	-89.9	4	03-06 (48)	2.4	55.5	138.7	47.9	Cropland/Natural
9	Tharandt	Germany	51	13.6	42	96-99 (42)	6.5	39.2	95.9	47.1	Evergreen forest
10	Sarrebourg	France	48.7	7.1	22	96-99 (32)	-0.1	32.8	102.3	42.7	Deciduous forest
11	Kennedy Oak, FL	USA	28.6	-80.7	18	02-06 (48)	6	49.1	120.3	40.4	Woody savanna
12	Loobos	Netherland	52.2	5.7	24	96-98 (30)	7.4	32.4	63.1	39.7	Evergreen forest
13	Sakaerat	Thailand	14.5	101.9	45	01-03 (32)	37.7	63.8	109.5	36.8	Tropical forest
Humid											
14	Norunda	Sweden	60.1	17.5	103	96-98 (29)	1.3	30.9	80.8	34	Evergreen forest
15	Fort Peck, MT	USA	48.3	-105.1	4	00-06 (84)	1.3	26	164	33	Grassland
16	Freeman, TX	USA	29.9	-98	3	05-08 (48)	6	49.1	120.3	30.9	Grassland
17	Little Washita, OK	USA	35	-98	3	96-98 (32)	8.9	41.6	104.4	30.7	Grassland
18	Mehrstedt 2	Germany	51.3	10.7	n/a	04-06 (34)	0	27	95.3	29.6	Grassland
Sub-humid											
19	Evora	Portugal	38.5	-8	28	05-05 (12)	-0.3	13.7	34.8	26.2	Savanna
20	Mauzac	France	43.4	1.3	3.5	05-07 (34)	8.3	37.2	91.4	25.5	Grassland
Mediterranean											
21	Bugac	Hungary	46.7	19.6	4	02-08 (72)	2.3	37.5	103.9	23.8	Cropland
22	Metolius, OR	USA	44.3	-121.6	12	04-08 (60)	2.3	30.3	71	22.8	Evergreen forest
23	Tonzi Ranch, CA	USA	38.4	-121	23	01-09 (80)	1.4	29.8	95.5	21	Woody savanna
24	Vaira Ranch, CA	USA	38.4	-121	2	01-09 (108)	-5.1	25.1	88	21	Woody savanna
Semi-arid											
25	Kherlenbayan	Mongolia	47.2	108.7	3.5	03-10 (68)	-2.3	10.5	50.8	17.5	Grassland
26	Llano de los Juanes	Spain	36.9	-2.8	2.8	05-05 (12)	7.2	18.7	36.7	15.4	Closed shrubland
27	Audubon, AZ	USA	31.6	-110.5	4	02-09 (87)	2	24.4	92.5	13.5	Open shrubland
28	Kendall, AZ	USA	31.7	-109.9	6.4	04-09 (68)	2.2	20.2	72.4	13.2	Grassland
29	Santa Rita, AZ	USA	31.8	-110.9	6.4	04-07 (48)	4.3	26	91.1	10.7	Open shrubland
Arid											
30	Corral Pocket, UT	USA	38.1	-109.4	1.9	01-07 (39)	4.6	14.8	33.3	9.8	Grassland
31	Sevilleta grass, NM	USA	34.4	-106.7	3	07-08 (19)	4.5	22.2	69.7	9	Grassland
32	Sevilleta shrub, NM	USA	34.3	-106.7	3	07-08 (24)	3.3	23.5	74.7	9	Grassland
33	Demokeya	Sudan	13.3	30.5	12	97-98 (17)	6.1	38.1	106.3	8.9	Grassland
34	Yatir	Israel	31.3	35.1	14	01-09 (48)	5.7	17.8	57.3	8.6	Open shrubland

770
771

772 Table 2. Average values of RMSE, BIAS and R^2 of actual ET estimates from the different complementary methods,
773 CRAE, AA and GG, for each climatic class.
774

Climatic class	RMSE (mm/month)			BIAS (mm/month)			R^2		
	CRAE	AA	GG	CRAE	AA	GG	CRAE	AA	GG
Very humid	27.6	29.0	22.6	15.8	12.2	10.6	0.73	0.71	0.73
Humid	31.2	35.2	27.1	19.2	16.5	14.3	0.77	0.73	0.75
Sub-humid	46.6	54.7	45.0	31.9	28.7	26.5	0.39	0.33	0.41
Mediterranean	35.3	58.1	47.4	18.6	28.8	25.3	0.51	0.42	0.45
Semi-arid	16.6	18.9	22.1	9.6	8.4	13.3	0.56	0.61	0.41
Arid	22.4	31.9	29.5	9.4	14.4	19.5	0.53	0.54	0.42
All classes	27.8	33.8	28.4	15.7	15.5	15.5	0.64	0.61	0.59

775
776
777

778

779

780 Table 3. Details of the 17 model variations developed based on the complementary relationships and the three
 781 original complementary methods.
 782

Criteria Equation	R _n		CR		α		β		G	
	R _T	R _{ASCE}	1	8	1.26	1.28	0.5	1.0	11	12
Value										
CRAE	✓		✓							
CR E1	✓			✓						
CRAE2		✓	✓							
CRAE3		✓		✓						
	✓		✓			✓		✓		
AA1	✓			✓		✓		✓		
AA2	✓			✓	✓		✓			
AA3		✓	✓			✓		✓		
AA4		✓		✓		✓		✓		
AA5		✓	✓		✓		✓			
AA6		✓		✓	✓		✓			
AA7	✓		✓		✓		✓			
GG	✓			✓				✓	✓	
GG1	✓		✓					✓	✓	
GG2	✓			✓				✓		✓
GG3	✓		✓					✓		✓
GG4		✓		✓				✓	✓	
GG5		✓	✓					✓	✓	
GG6		✓		✓				✓		✓
GG7		✓	✓					✓		✓

783

784

785

786

787

788 Table 4. Sixteen GG-based model variations developed given that ETW is calculated using ET_{PT} equation.
 789

Criteria	R _n		Complementary Relationship		α		G	
	Equation	Value	1	8	1.26	1.28	11	12
		R _T R _{ASCE}						
GG8	✓		✓		✓			✓
GG9	✓			✓	✓			✓
GG10	✓		✓		✓		✓	
GG11	✓			✓	✓		✓	
G12	✓		✓			✓	✓	
GG13	✓			✓		✓	✓	
GG14	✓		✓			✓		✓
GG15	✓			✓		✓		✓
GG1		✓	✓			✓		✓
GG17		✓		✓		✓		✓
G 18		✓	✓			✓	✓	
GG19		✓		✓		✓	✓	
GG20		✓	✓		✓		✓	
GG21		✓		✓	✓		✓	
GG22		✓	✓		✓			✓
GG23		✓		✓	✓			✓

790

791

792 Table 5. Results of the performance of different models in a given climatic class described through the best values of
 793 RMSE, BIAS and R^2
 794

Metric	Climatic class						All classes
	Very humid	Humid	Sub-humid	Mediterranean	Semi-arid	Arid	
RMSE	GG3	GG7	GG22	GG22	GG20	GG20	GG22
BIAS	GG1	GG7	GG20	GG22	GG14	GG14	GG18
R^2	GG17 & GG23	GG11 & GG13	GG18 & GG20	GG18 & GG20	GG17 & GG23	GG18 & GG20	GG18 & GG20

795

796

797 Table 6. Comparison of performance of GG18 to the most recently published ET studies.

Citation	Method	# of sites	RMSE (mm/month)			BIAS (mm/month)			R ²		
			min	max	mean	min	max	mean	min	max	mean
Present study	GG18	34	10.3	59.9	20.6	0.5	58.1	10.6	0.01	0.94	0.64
Suleiman and Crago (2004)	Radiometric surface temperature	2	32.0	53.4					0.78	0.94	
Mu et al. (2007)	Revised remote sensing and Penman-Monteith	19	7.7	56.4	29.2	2.9	41.1	15.6	0.13	0.96	0.76
Szilagyi and Kovacs (2010)	CRAE method	3	2.6	39.7	15.3	0.0	21.0	8.4	0.79	0.95	0.85
Han et al. (2011)	Enhanced GG method	4	3.7	16.0	10.7				0.82	0.98	0.92
Huntington et al. (2011)	Modified AA method	5			11.0						0.71
Mu et al. (2011)	Modified remote sensing and Penman-Monteith	46	9.4	52.0	25.6	0.3	28.6	10.0	0.02	0.93	0.65
Thompson et al. (2011)	Penman-Monteith and soil moisture model	14	34.0	175.0	94.1						

798

799

800

801 **Figure Captions**

802 Figure 1. A schematic representation of the complementary relationship between ET, ETW and
803 ETP (after Morton, 1983).

804 Figure 2. Map showing the locations of the 34 EC sites with measured ET flux data.

805 Figure 3. Anomalies of RMSE, BIAS and R^2 values for 17 model variations across the 34 sites.
806 Here anomalies are computed based on the values computed with each corresponding
807 complementary method.

808 Figure 4. Boxplots of RMSE, BIAS and R^2 metrics of the seven promising model variations for
809 the simplified climatic classes.

810 Figure 5. Scatter plots of average ET estimates (mm/month) for GG18, GG20 and GG22 model
811 variations in comparison to measured ET_{EC} fluxes from 33 sites (all except site 4) in the wet
812 (triangle), moderate (circle) and dry (square) climatic classes.

813

814 Figure 6. RMSE, BIAS and R^2 of the GG18 model variation at each site in the wet (triangle),
815 moderate (circle) and dry (square) climatic classes and the dashed lines indicate the average
816 values.

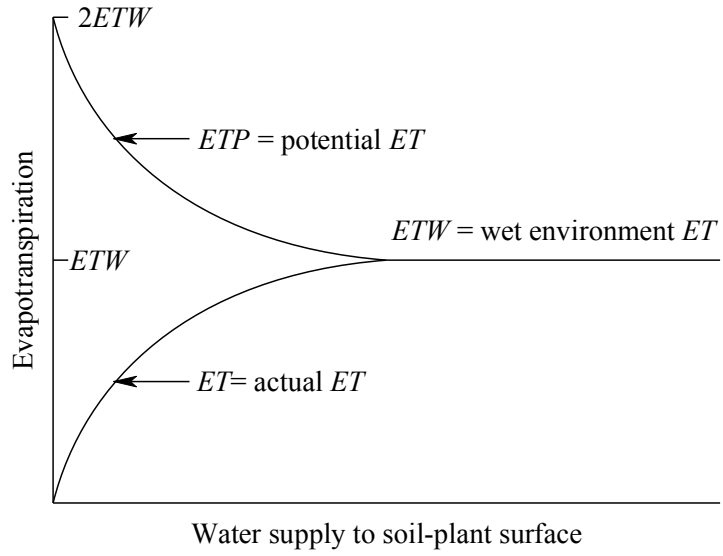
817 **Figure 7. Schematic showing the structure of the proposed GG18 model.**

818

819

820 **Figures**

821



822 Figure 1. A schematic representation of the Complementary relationship between ET, ETW, and ETP (after Morton,
823 1983).

824

825



826

827 Figure 2. Map showing the locations of the 34 EC sites with measured ET flux data.

828

829

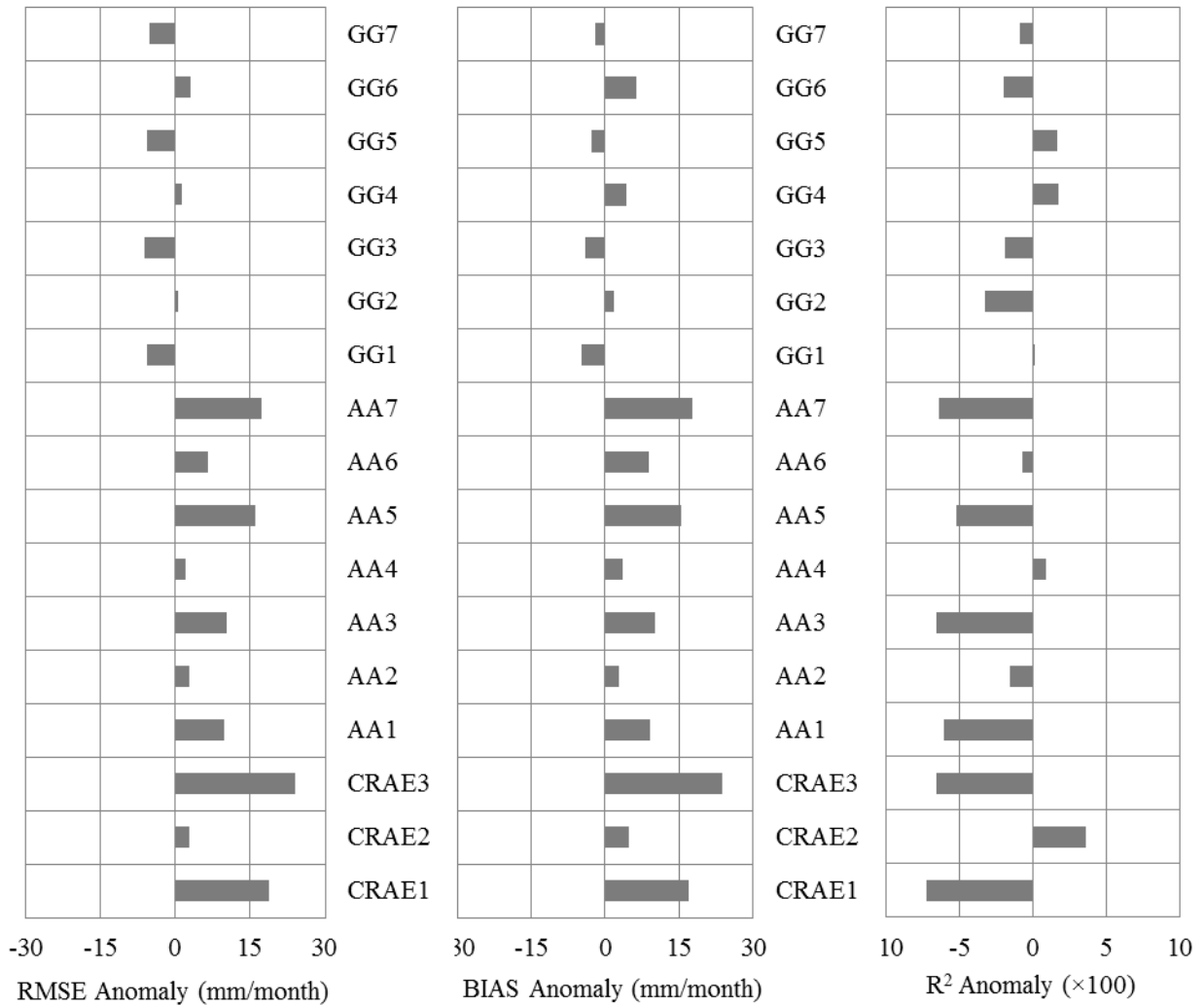
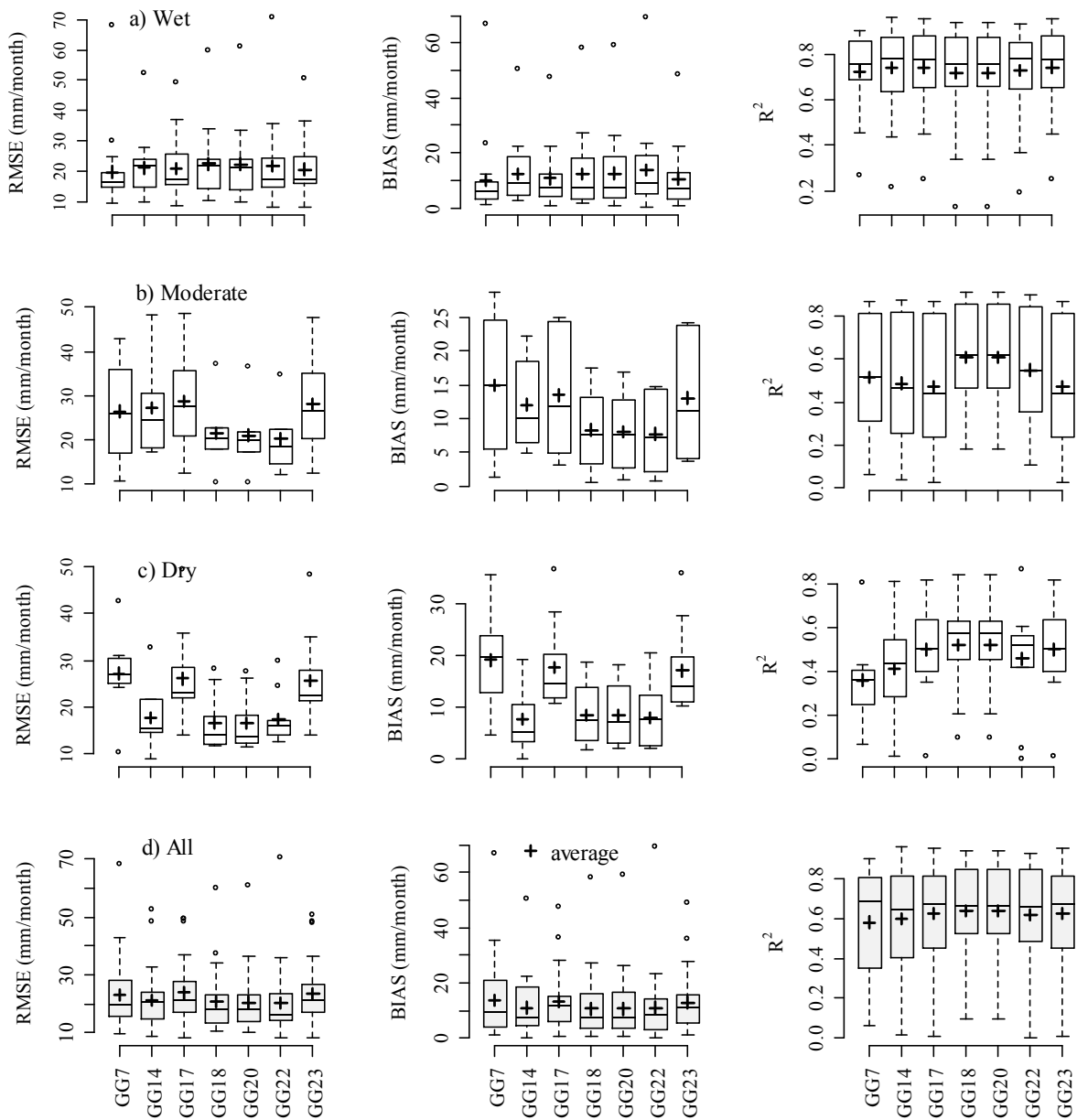


Figure 3. Anomalies of RMSE, BIAS, and R^2 values for 17 model variations across the 34 sites. Here anomalies are computed based on the values computed with each corresponding Complementary method.

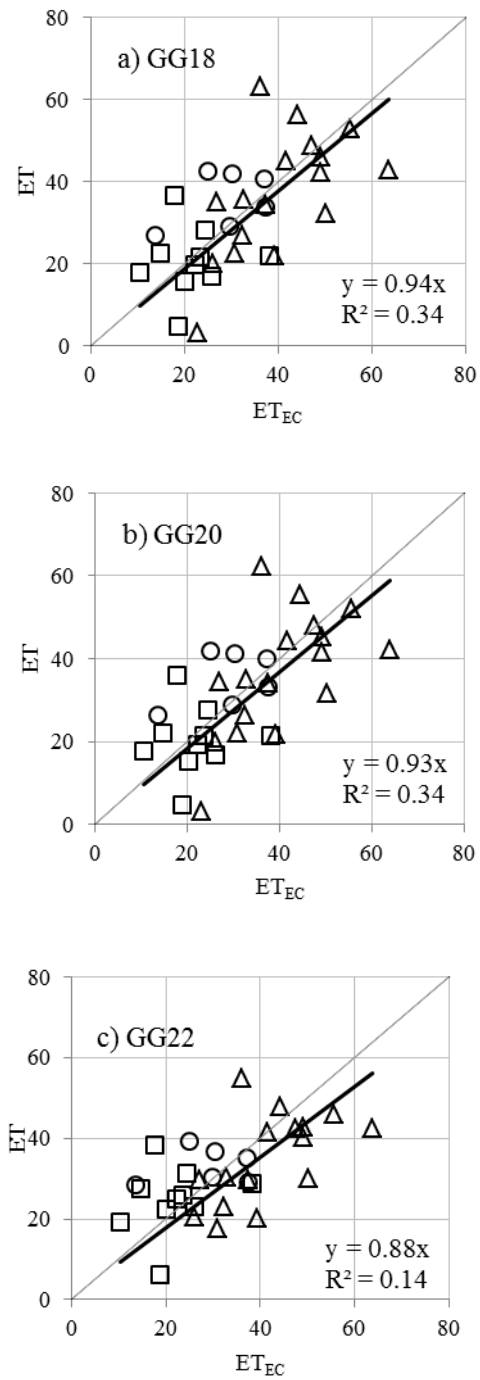
830



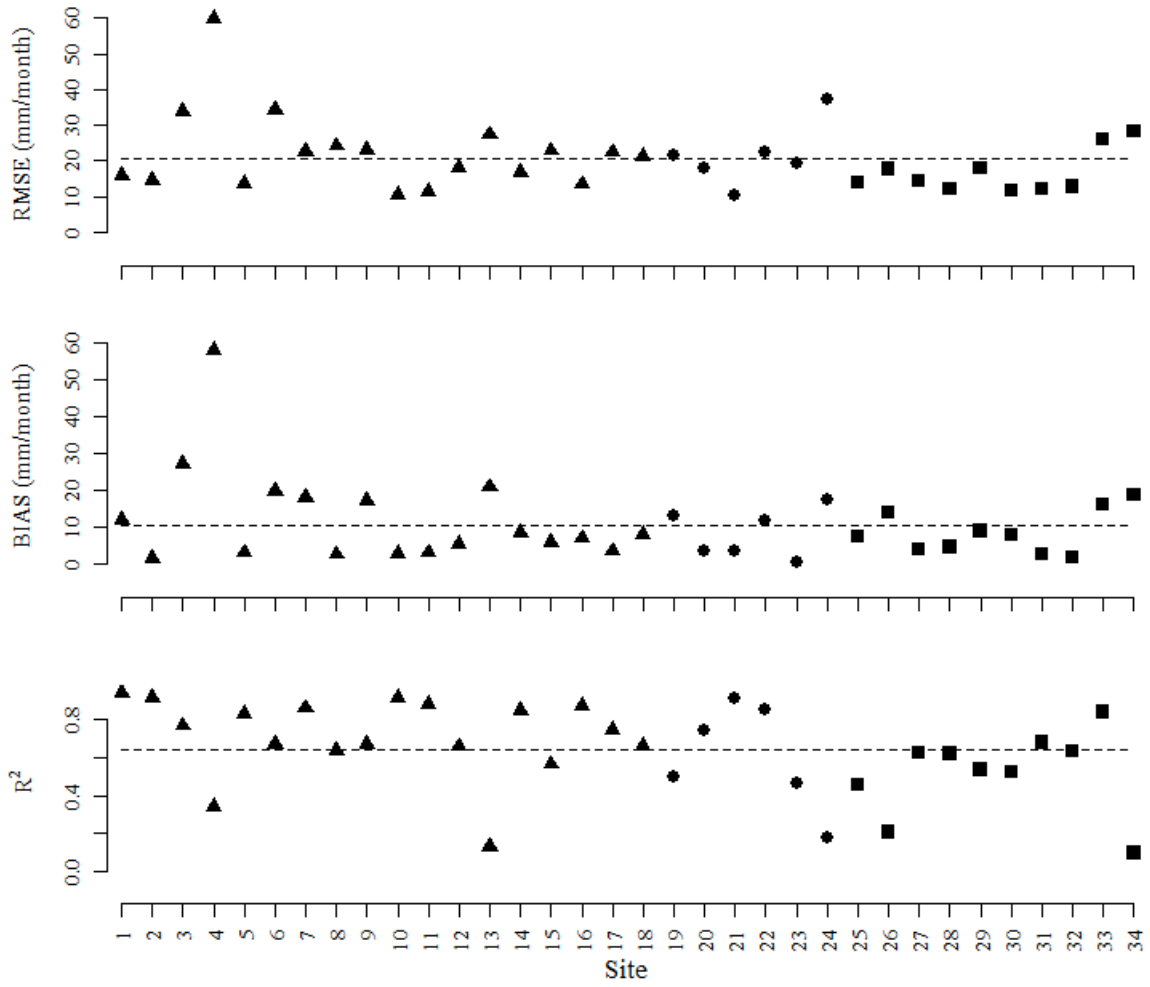
831

832 Figure 4. Boxplots of RMSE, BIAS, and R² metrics of the seven promising model variations for the simplified
 833 climatic classes.

834



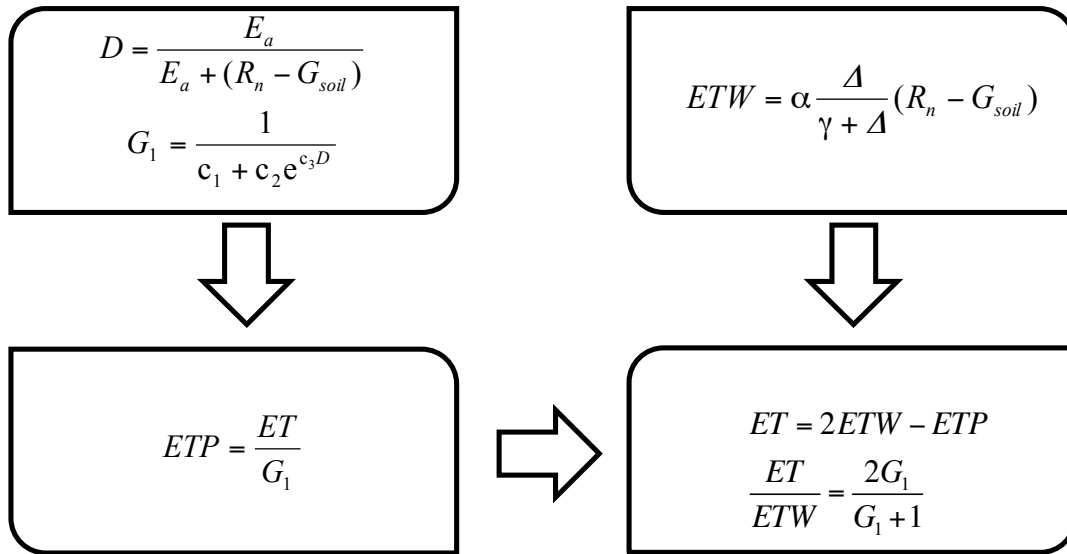
836 Figure 5. Scatter plots of average ET estimates (mm/month) for GG18, GG20, and GG22 model variations in
 837 comparison to measured ET_{EC} fluxes from 33 sites (all except site 4) in the wet (triangle), moderate (circle), and dry
 838 (square) climatic classes.
 839



841 Figure 6. RMSE, BIAS, and R² of the GG18 model variation at each site in the wet (triangle), moderate (circle), and
 842 dry (square) climatic classes and the dashed lines indicate the average values.

844

845



846

847 Figure 7. Schematic showing the structure of the proposed GG18 model.

848

849